Preparation, Characterization, and Physical Properties of the Series MPd_3S_4 (M = Rare Earth)

Douglas A. Keszler and James A. Ibers *
Department of Chemistry, Northwestern University, Evanston, Illinois 60201, U.S.A.
Melvin H. Mueller
Materials Science Technology Division, Argonne National Laboratory, Argonne, Illinois 60439, U.S.A.

The synthesis, characterization, and physical properties of the ternary sulphides MPd_3S_4 (M = rare-earth metal) are described. The material $LaPd_3S_4$ has the ideal $NaPt_3O_4$ structure as deduced from *X*-ray and neutron diffraction results. Comparisons between the isomorphous sulphides and oxides are presented.

The platinum bronzes[1] $M_xPt_3O_4$, where M = Na, Ca, Ni, Cd, *etc.*, are metallic phases with considerable non-stoicheiometry of the ternary element M ($0 \leqslant x \leqslant 1$). In contrast, the analogues MPd_3O_4,[2] where M = Ca or Ba, are semiconducting and deviation from stoicheiometry of the ternary element M has not been demonstrated.

In an earlier communication[3] we reported the preparation of the first sulphides MPd_3S_4 (M = rare-earth metal) analogous to these oxide materials. Here we present additional details concerning these sulphides and offer comparisons of structure and physical properties with the oxides.

Our interest in the ternary sulphides derives in part from the physical properties of the platinum bronzes and their use as catalysts for reduction of organic compounds,[4] H_2–O_2 fuel-cell electrocatalysts,[5] and chlor-alkali anodes.[6] In addition, the preparation of the sulphide analogues is of interest as the simple binary platinum-metal sulphides have been studied for hydrodesulphurization processes[7] and for the synthesis of aromatic amines.[8]

Experimental

Synthesis of MPd_3S_4 (M = Y, La, Ce, Pr, Sm, Tb, Ho, *or* Er).—Each phase was prepared by reaction of a stoicheiometric mixture of the elements (purity ⩾99.9%). The compound $CePd_3S_4$ was obtained only when *ca.* 1 atom % I_2 was added as a mineralizer to the mixture of the elements. The reactions were performed in sealed, evacuated silica tubes that were lined with carbon through pyrolysis of toluene. The contents of each tube were heated at 1 125 K for *ca.* 3 weeks with intermediate grindings every 4 d. After the final period of heating the charges were reground and passed through a 270-mesh screen. In order to reduce the concentration of adventitious oxygen the powder was then treated under a flow of CS_2 at 700 K for 2 h, reground under a nitrogen atmosphere, and again treated with CS_2 for an additional 2 h. Chemical analysis by fast neutron activation, as performed at IRT Corporation, indicates that this CS_2 treatment affords an oxygen content of less than 0.15 wt. %. The samples are single phases as determined through analysis of *X*-ray powder diffraction data.

For MPd_3S_4 (M = Eu, Yb, or Th), the products have not been obtained as single phases by reaction of the elements. However, the *X*-ray powder diagrams contain reflections consistent with a $NaPt_3O_4$ structural type.

The phases MPd_3S_4 (M = La, Ce, Pr, or Sm) were also prepared in *ca.* 95% yield with use of the appropriate iodide MI_3 as a promoter.[9] The reactions were performed in vitreous carbon crucibles that were contained in sealed, evacuated silica tubes. The charges were heated at 1 125 K for 18 h. A given tube was cooled and then opened under a nitrogen atmosphere. The product was thoroughly washed with dimethylformamide and dried. It was then isolated as a fine free-flowing powder. Analysis of *X*-ray powder patterns consistently revealed the presence of weak reflections attributable to the impurity M_2O_2S. Extension of the period of heating afforded a lower yield of the desired phase. The impurity probably arises from attack of $MI_3(g)$ on the walls of the silica container and subsequent reaction with metal sulphide or sulphur.[10] Attempts to prepare pure single-phase material by lining the silica tube with carbon were not successful. Furthermore, preparations with the use of low-melting eutectics, such as KI–MI_3, have thus far proven unsuccessful.

Attempts to prepare the material $Ce_{0.75}Pd_3S_4$ always afforded the phase $CePd_3S_4$. In addition, synthesis of the phases MPd_3S_4 where M = Sc, In, Bi, or Ta has not been realized.

X-*Ray Diffraction.*—*X*-Ray powder diffraction data were obtained with nickel-filtered Cu-K_α radiation on a Rigaku Geigerflex powder diffractometer. Experimental traces were compared with those generated by a local version of the program LAZY-PULVERIX.[11] The unit-cell parameter *a* was determined from a weighted least-squares analysis of several high-angle reflections in the range $114 < 2\theta < 153°$ [λ(Cu-K_{α_1}) = 1.540 562 Å]. The position of the K_{α_1} member of each doublet was determined from digitized data obtained by step scanning [100 s, 0.01° (2θ)] each reflection. National Bureau of Standards Si Powder Standard Reference Material 640a[12] was used as an internal standard.

Magnetic Susceptibility Measurements.—Static magnetic susceptibility data were obtained with an S.H.E. VTS-10 SQUID susceptometer. The calibration of the instrument was monitored with $HgCo(SCN)_4$ and the superconducting transition of niobium metal. All measurements were performed at 7.5 kG (0.75 T) with the samples contained in a closed silica bucket. Approximately 25 min were allowed for sample equilibration at each temperature. The data were analysed with a local package of computer programs.[13]

Electrical Conductivity.—The electrical conductivity measurement was made on a pressed pellet with the four-probe van der Pauw technique, as described elsewhere.[14] Simple pressing of the powder invariably resulted in cracked pellets; therefore several drops of water were added to the powder prior to pressing. The pellet was then sintered for several days at 1 100 K.

Neutron Diffraction Measurements.—Neutron diffraction data for $LaPd_3S_4$ powder were collected in the back-scattering detector banks of the general-purpose powder diffractometer of the IPNS facility at Argonne National Laboratory.[15] The

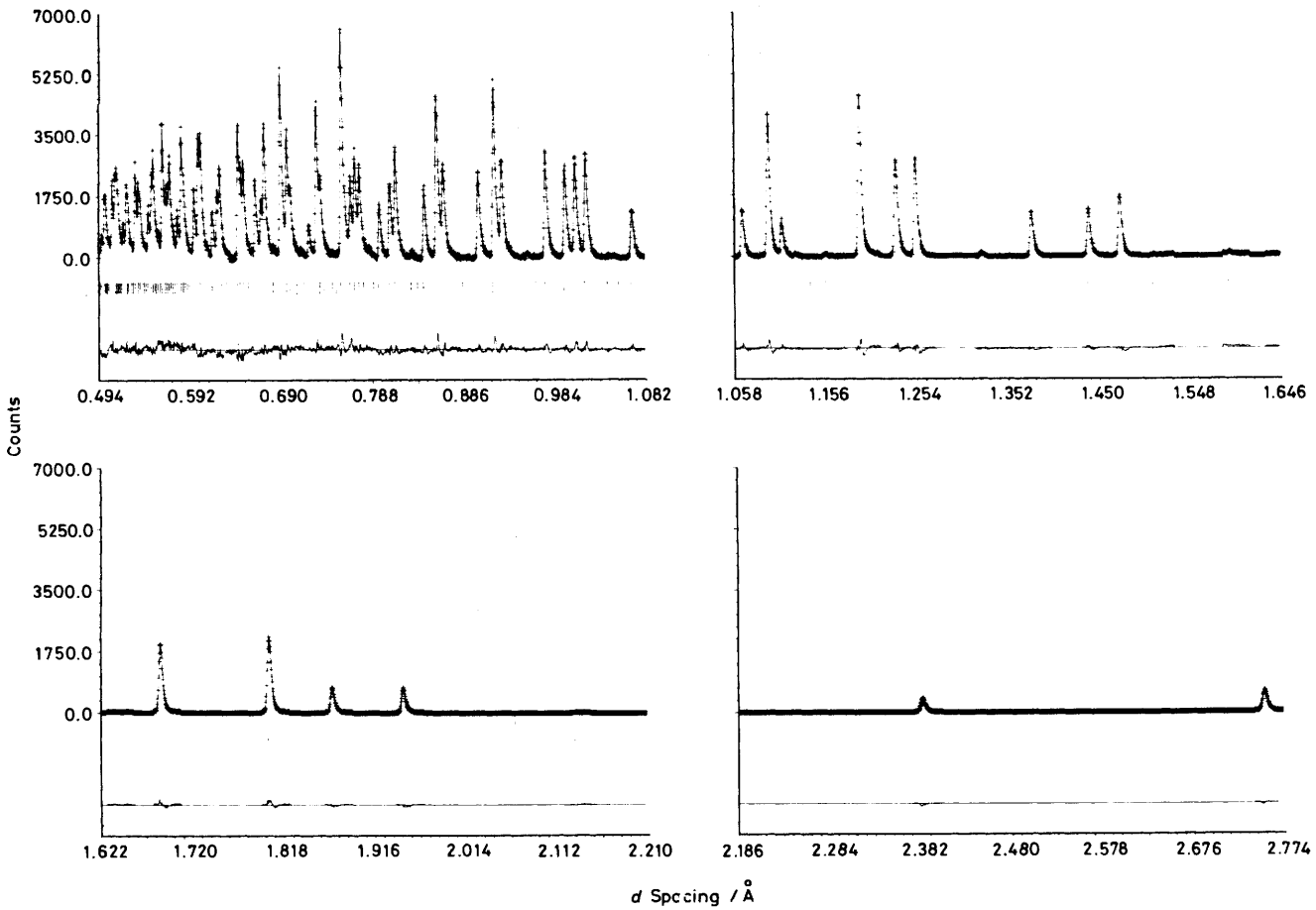

Figure 1. Final Rietveld refinement profile for $LaPd_3S_4$. (+) Data points; (——) calculated profile; vertical lines below the profile indicate the positions of all allowed reflections. The background has been removed before plotting. A difference plot appears at the bottom of each frame

powder data were refined with use of a Rietveld profile-analysis code that has been modified for time-of-flight data from spallation pulsed neutron sources.[16] From *X*-ray diffraction powder data we determined that the phase $LaPd_3S_4$ is of the general $NaPt_3O_4$ structural type. No additional reflections unrelated to this structural type were observed in the neutron data. The space group for the present material then is either O_h^3-*Pm3n* or T_d^4-$P\bar{4}3n$, based on the systematic extinction *hhl*, $l = 2n + 1$. In space group *Pm3n* the S position is $(\frac{1}{4},\frac{1}{4},\frac{1}{4})$; in space group $P\bar{4}3n$ it is (x,x,x). Otherwise the structures are identical in the two groups. Refinement with $x \neq \frac{1}{4}$ afforded higher agreement indices. We therefore assume the structure to be centrosymmetric. The occupancy of the La atom was varied and showed no deviation from unity. Refinement of the defect model $La_{0.89}\square_{0.11}Pd_{2.67}\square_{0.33}S_4$ also afforded an increased residual, $R_{wp} = 0.064$. The final refinement in space group O_h^3-*Pm3n* included 4 940 data points (representing 5 μs-wide time channels) and 140 allowed reflections. The 11 parameters refined included isotropic thermal parameters, cell constants, a scale factor, and background and profile parameters.* The best-fit profile is provided in Figure 1.

Results and Discussion

As determined through the structural investigation, the material $LaPd_3S_4$ is of the ideal $NaPt_3O_4$ structural type. A drawing of this structure appears in Figure 2. Metrical data for each member of the series MPd_3S_4 are given in Table 1. These data have been derived from the isometric unit-cell parameter *a* on the assumption that each material has the ideal $NaPt_3O_4$ structure.

Prior to analysing these data, it is instructive to consider an 'ideal' Pd_3S_4 substructure. As seen in Figure 2 the structure of $LaPd_3S_4$ consists of three orthogonal chains of palladium-centred face-to-face square planes of S atoms (Pd_3S_4). Encapsulated within these chains is the eight-fold cubic co-ordination site of the La atom. If a Pd–S distance of 2.325 Å [17] is assumed for the Pd_3S_4 substructure, then the distances 2.848 and 3.288 Å result for the ideal M–S and S–S distances, respectively. Considering now Table 1, we see that for each compound the Pd–S distance is greater than the predicted value. The distance provides structural evidence that these materials are indeed sulphides rather than oxides; this result is consistent with the neutron activation analysis. Also seen in Table 1 are distances M–S for the lighter congeners that are less than those predicted from radii values, and distances for the heavier members that are slightly greater than the predicted values. The short M–S distances for the larger ions are a measure of the geometrical and bonding constraints of the structure. For our ideal Pd_3S_4 network we calculate a M–S distance of 2.848 Å, which corresponds closely with M = Er. To accommodate a

* Refinement data for $LaPd_3S_4$: space group O_h^3-*Pm3n*; $a = 6.739\,4(1)$ Å; $0.50 \leq d \leq 2.82$ Å; La(2a), 0,0,0, $B = 0.33(1)$ Å^2; Pd(6d), $\frac{1}{4},\frac{1}{2},0$, $B = 0.475(1)$ Å^2; S(8e), $\frac{1}{4},\frac{1}{4},\frac{1}{4}$, $B = 0.30(1)$ Å^2; $R_p = 0.031$, $R_{wp} = 0.050$, $R_B = 0.056$ (see ref. 15 for definitions of agreement indices).

Table 1. Structural data for the series MPd_3S_4

Compound	a/Å	M–S/Å	Pd–S/Å	S–S/Å	Crystal radius* of M^{III}/Å
$LaPd_3S_4$	6.739 8(1)	2.918 4(1)	2.382 9(1)	3.369 9(1)	1.300
$CePd_3S_4$	6.713 0(1)	2.906 8(1)	2.373 4(1)	3.356 5(1)	1.283
$PrPd_3S_4$	6.698 9(1)	2.900 7(1)	2.368 4(1)	3.349 5(1)	1.266
$SmPd_3S_4$	6.669 2(1)	2.887 8(1)	2.357 9(1)	3.334 6(1)	1.219
$EuPd_3S_4$	6.675(3)	2.890(1)	2.360(1)	3.338(2)	1.206
YPd_3S_4	6.634 9(1)	2.873 0(1)	2.345 8(1)	3.317 5(1)	1.159
$HoPd_3S_4$	6.634 6(1)	2.872 9(1)	2.345 7(1)	3.317 3(1)	1.155
$ErPd_3S_4$	6.624 0(1)	2.868 3(1)	2.341 9(1)	3.312 0(1)	1.144

* Crystal radii for co-ordination number 8 are taken from ref. 17. Other relevant radii are: Pd^{II}, 0.625; S^{-II}, 1.70 Å.

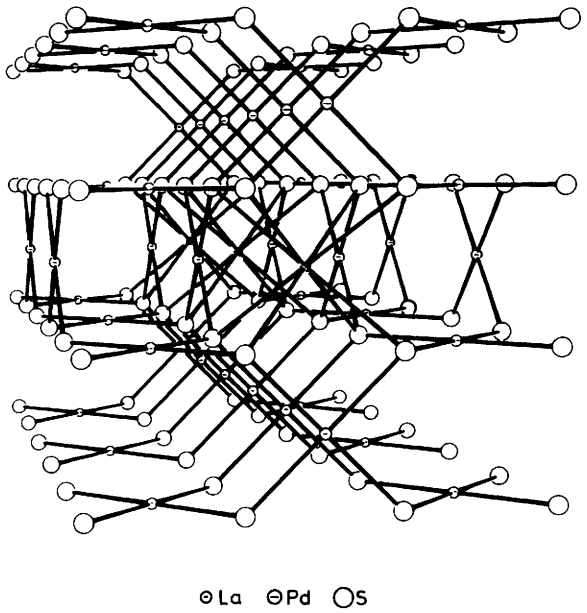

Figure 2. Drawing of the $LaPd_3S_4$ structure. The eight-co-ordinate La atoms are in the centre of the Figure

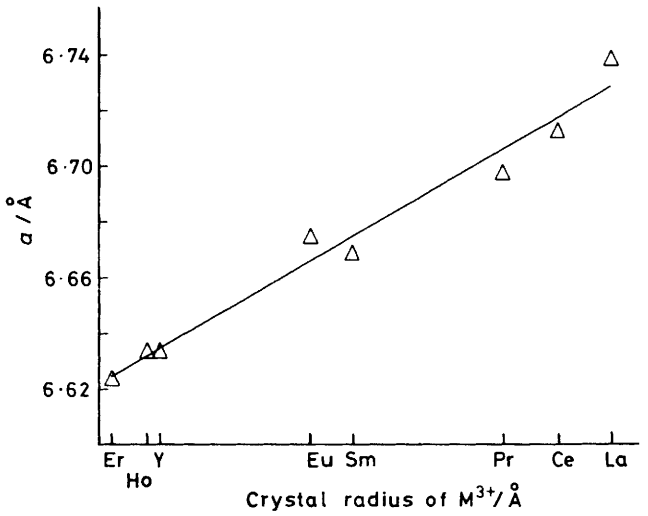

Figure 3. Lattice parameter a *vs.* crystal radius of M^{III}. The radius scale is given in Table 1

larger ion, for example La^{3+}, the structure must expand and the distances La–S 2.918 4(1) Å and Pd–S 2.382 9(1) represent a compromise in the shortening and lengthening, respectively, of the predicted values for formation of the compound. The large Pd–S and M–S distances for the smaller M members may arise from increased S • • • S non-bonded interactions that would occur with shorter S • • • S distances.

A plot of the unit-cell parameter a *vs.* M^{III} crystal radius is given in Figure 3. The cell parameter exhibits a monotonic decrease with decreasing crystal radius. The data are consistent with the assignment of Ce^{III}, Eu^{III}, and Sm^{III} in $CePd_3S_4$, $EuPd_3S_4$, and $SmPd_3S_4$, respectively.

The results of the magnetic measurements are summarized in Figures 4—6 and in Table 2. For the heavier rare-earth materials $TbPd_3S_4$ and $HoPd_3S_4$, the linear portion of the curve of reciprocal molar susceptibility, χ_M^{-1} (e.m. units mol^{-1}), *vs.* temperature fitted the expression $\chi_M = C/(T - \theta_P)$. Paramagnetic moments per formula unit $\mu_{eff.} = 2.83C^{\frac{1}{2}}\beta$, calculated from the Curie–Weiss constant, C, with extrapolated Curie–Weiss temperatures, θ_P, are listed in Table 2. The susceptibility data for the ceric rare earths (Pr, Sm) cannot be described by a simple Curie–Weiss law. The magnetic behaviour of $PrPd_3S_4$ closely resembles that for the ceric analogues of

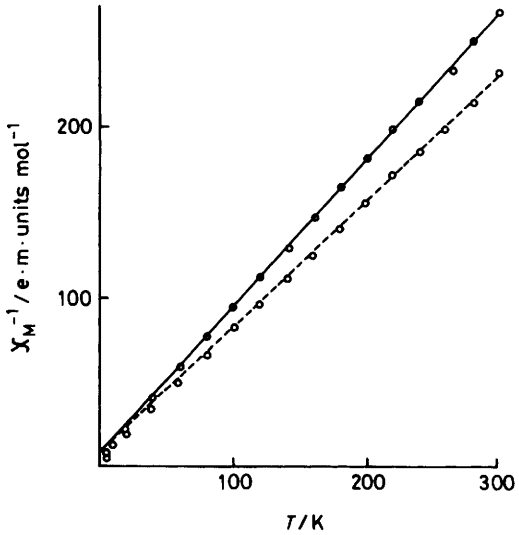

Figure 4. Reciprocal molar susceptibility *vs.* temperature for $TbPd_3S_4$ (——) and $HoPd_3S_4$ (– – – –)

MMo_6S_8.[18] As both materials form with similar environments about the rare-earth metal ion, the similar magnetic behaviours may be ascribed to crystal-field effects. The data for the

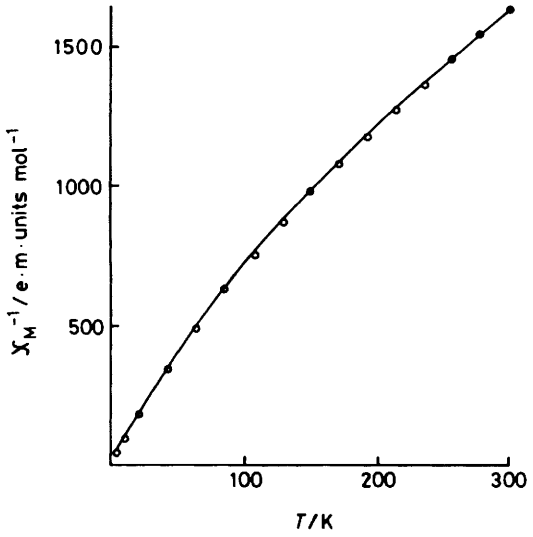

Figure 5. Reciprocal molar susceptibility *vs.* temperature for $PrPd_3S_4$

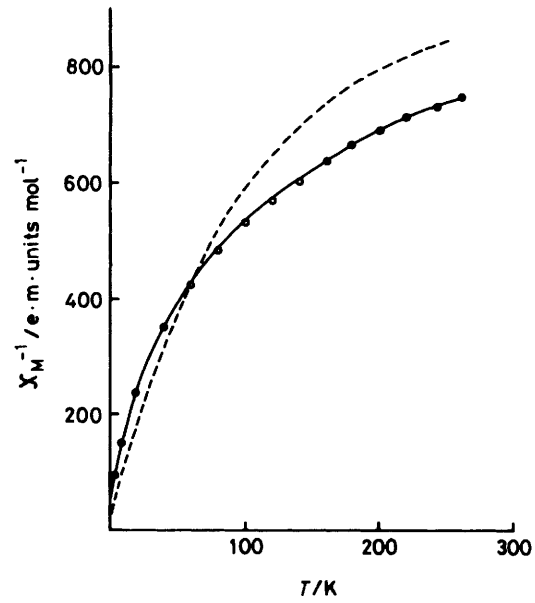

Figure 6. Reciprocal molar susceptibility *vs.* temperature for $SmPd_3S_4$ (– – – –, theoretical; ——, experimental)

Table 2. Magnetic data for ternary rare-earth metal sulphides

Compound	θ_P/K	$\mu_{eff.}$ Exptl.	$\mu_{eff.}$ Calc. (M^{III})
$PrPd_3S_4$	—	3.66	3.58
$SmPd_3S_4$	—	1.66*	1.55*
$TbPd_3S_4$	−9	9.64	9.74
$HoPd_3S_4$	−10	10.44	10.60

* At 260 K.

samarium analogue are in good agreement with the theory of closely spaced multiplets for Sm^{III}.[19] The behaviour expected for the free ion Sm^{III} has been included in Figure 6 for comparison. The observation of Sm^{III} is also consistent with the lattice parameter *a* as seen in Figure 3.

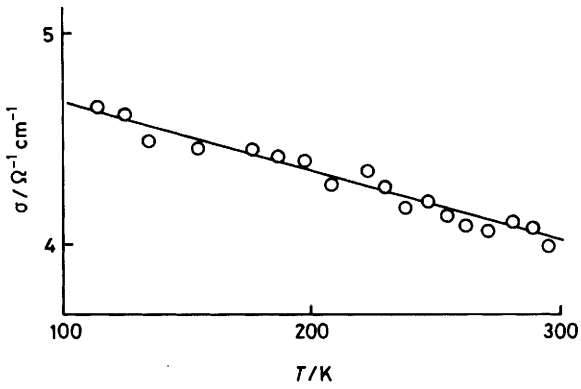

Figure 7. Electrical conductivity *vs.* temperature for $LaPd_3S_4$

The experimentally derived paramagnetic effective moments for the phases MPd_3S_4 are in close agreement with theoretical values for free M^{III} ions, as calculated from Hund's rules. Therefore, at least at higher temperatures, the paramagnetic behaviour of these materials derives largely from the M atoms. This is supported by magnetic measurements for YPd_3S_4 that reveal only very weak paramagnetism.

Electrical conductivity data obtained from a pressed pellet of $LaPd_3S_4$ are illustrated in Figure 7. Because of the method used, we view the results of this measurement with some reservation. The behaviour is that expected for a metallic conductor. This conclusion is based on the room-temperature value of the conductivity and the small positive temperature coefficient with decreasing temperature.

The lack of a partial occupancy of the rare-earth metal site in the sulphide materials follows a behaviour similar to that of the palladium oxides ($CaPd_3O_4$). This contrasts with the materials $M_xPt_3O_4$ (M = Na, Ni, *etc.*), where the presence of a band resulting from Pt–Pt interactions allows a variation in *x*. Indeed the binary material Pt_3O_4 is known whereas Pd_3O_4 and Pd_3S_4 are not. From the current results then a simple valence description is: M^{III}, Pd^{II}, S^{-II}. The compounds are thus formulated as $[(MPd_3S_4) + e^-]$. This model then represents a departure from the partially *oxidized* nature of the metallic materials, $M_xPt_3O_4$.[20] Although an extended homogeneity range cannot be excluded, the present neutron diffraction and electrical conductivity results are consistent with a partially *reduced* nature for the sulphides. In view of the non-existence of the materials $InPd_3S_4$ and $BiPd_3S_4$, the energetic requirements for formation of the phases MPd_3S_4 are also consistent with the model. Further analyses and especially the preparation of single crystals will afford a better understanding of this class of new and interesting materials.

Acknowledgements

This research was supported in part by the U.S. Department of Energy. Some of the measurements were made in the Magnet and *X*-ray Facilities of Northwestern University's Materials Research Center, supported in part under the NSF-MRL programme. We thank Nathaniel Brese for the determination of the lattice parameter of the phase $EuPd_3S_4$.

References

1 J. Waser and E. D. McClanahan, *J. Chem. Phys.*, 1951, **19**, 413; 1952, **20**, 199; D. Cahen, J. A. Ibers, and R. D. Shannon, *Inorg. Chem.*, 1972, **11**, 2311; D. Cahen, J. A. Ibers, and M. Mueller, *ibid.*, 1974, **13**, 110; K. B. Schwartz, C. T. Prewitt, R. D. Shannon, L. M. Corliss, and B. Chamberland, *Acta Crystallogr., Sect. B*, 1982, **38**, 363.
2 R. C. Wnuk, T. R. Touw, and B. Post, *IBM J. Res. Dev.*, 1964, **8**, 185.

3 D. A. Keszler and J. A. Ibers, *Inorg. Chem.*, 1983, **22**, 3366.
4 D. Cahen and J. A. Ibers, *J. Catal.*, 1973, **31**, 369.
5 R. D. Shannon, T. E. Gier, P. F. Carcia, P. E. Bierstedt, R. B. Flippen, and A. J. Vega, *Inorg. Chem.*, 1982, **21**, 3372.
6 G. Thiele, G. Zöllner, and K. Koziol, B.P. 1 328 270/1973; U.S.P. 4 042 484/1977; K. Koziol, H-H. Sieber, and H. S. Rathjen, U.S.P. 3 948 752/1976; D. Zöllner, C. Zöllner, and K. Koziol, U.S.P. 3 962 068/1976; C. Zöllner, D. Zöllner, and K. Koziol, U.S.P. 3 992 280/1976; M. Fukuda and K. Asai, G. P. 1 671 455/1975; G. Thiele, D. Zöllner, and K. Koziol, G.P. 1 813 944/1975.
7 T. A. Pecoraro and R. R. Chianelli, *J. Catal.*, 1981, **67**, 430.
8 F. S. Dovell and H. J. Greenfield, *J. Am. Chem. Soc.*, 1965, **87**, 2767.
9 W. Kwestroo, in 'Preparative Methods in Solid State Chemistry,' ed. P. Hagenmuller, Academic Press, New York, 1974, p. 563.
10 G. Meyer, *Prog. Solid State Chem.*, 1982, **14**, 191.
11 K. Yvon, W. Jeitschko, and E. Parthé, *J. Appl. Crystallogr.*, 1977, **10**, 73.
12 C. R. Hubbard, *J. Appl. Crystallogr.*, 1983, **16**, 285.
13 D. A. Keszler and S. A. Sunshine, SQUIMAG, Program for reduction, least-squares analysis, and graphical display of magnetic data, Northwestern University, 1983.
14 D. Cahen, J. R. Hahn, and J. R. Anderson, *Rev. Sci. Instrum.*, 1973, **44**, 2567.
15 J. D. Jorgensen and F. J. Rotella, *J. Appl. Cyrstallogr.*, 1982, **15**, 27.
16 R. B. Von Dreele, J. D. Jorgensen, and C. G. Windsor, *J. Appl. Crystallogr.*, 1982, **15**, 581.
17 R. D. Shannon, in 'Structure and Bonding in Crystals,' vol. 2, eds. M. O'Keefe and A. Navrotsky, Academic Press, New York, 1981, p. 53; R. D. Shannon, *Acta Crystallogr., Sect. A*, 1976, **32**, 751.
18 M. Pelizzone, A. Treyvaud, P. Spitzli, and Ø. Fischer, *J. Low. Temp. Phys.*, 1977, **29**, 453.
19 J. H. Van Vleck, 'The Theory of Electric and Magnetic Susceptibilities,' Clarendon Press, Oxford, 1932.
20 D. Cahen, J. A. Ibers, and J. B. Wagner, jun., *Inorg. Chem.*, 1974, **13**, 1377.

Received 13*th December* 1984; *Paper* 4/2116